Structural Characterization, *In Silico* Studies and *In Vitro* Antibacterial Evaluation of a Furanoflavonoid from Karanj

Anuma Singh[1], **Iffat Jahan**[1], **Mrinal Sharma**[1], **Latha Rangan**[1], **Alika Khare**[2], **Aditya N Panda**[3]

[1] Department of Biosciences and Bioengineering, Indian Institute of Technology Guwahati, Guwahati, Assam, India
[2] Department of Physics, Indian Institute of Technology Guwahati, Guwahati, Assam, India
[3] Department of Chemistry, Indian Institute of Technology Guwahati, Guwahati, Assam, India

Abstract

Pongamia pinnata, popularly referred to as Karanj, is a multipurpose legume well known for its traditional and pharmacological properties with an efficient remedy for human health problems. Karanjin, a furanoflavonoid (3-methoxy-2-phenylfuro [2,3-h] chromen-4-one), is the main constituent of Karanj seeds with important biological attributes. The present investigation was aimed at standardizing a process for the isolation of karanjin from seed oil with an emphasis on achieving a higher yield of the pure compound. Structural elucidation and characterization were carried out via HRMS, Fourier transform infrared spectroscopy, X-rays diffraction, NMR, Raman spectroscopy, and thermogravimetric studies. The optimized geometry of the karanjin compound has been determined by a density functional theory and compared with experimental values, which are in excellent agreement. The potency of karanjin against pathogenic indicators was evaluated and confirmed by Raman scattering and field emission scanning electron microscopy imaging. The physicochemical parameters of karanjin were determined by *in silico* drug likeness properties, and molecular docking was also performed, which revealed the potential of karanjin as a highly functionalized and medicinally useful compound. From the docked conformations, the carbonyl group, 3-methoxy group, and oxygen atom in the C ring of the karanjin molecule were found to be biologically important for hydrogen bond formation with common bacterial enzymes involved in fatty acid biosynthesis. The mode of antibacterial action of karanjin revealed the complex patterns of probable cell wall disruption. This is the first report with regard to karanjin characterization and theoretical calculations of a density functional theory and its utility as a potential pharmacophore depicting an antibacterial property using Raman spectroscopy and docking studies.

Key words
Pongamia pinnata · Fabaceae · antibacterial activity · furanoflavonoid · Karanj · Raman spectroscopy

Abbreviations

DFT:	density functional theory
FESEM:	field emission scanning electron microscopy
FTIR:	Fourier transform infrared spectroscopy
TGA:	thermogravimetric analysis
XRD:	X-rays diffraction

Supporting information available online at http://www.thieme-connect.de/products

Pongamia pinnata L. (Fabaceae) or Karanj is a perennial, multipurpose, medium-sized leguminous tree, also well known for its traditional and pharmacological properties with an efficient remedy for human health problems. Seed oil of Karanj contains 5–6% of flavonoids such as karanjin, kanjone, pongaglabrone, and pongapin, out of which the main constituent is karanjin. Karanjin, a furanoflavonoid (3-methoxy-2-phenylfuro [2, 3-h] chromen-4-one), is the main constituent of Karanj seeds, possessing various important biological attributes. Its isolation and extensive characterization will definitely be helpful in understanding its mode of action in various aspects of pharmacology and therapeutics.

A number of studies have been carried out regarding the structural elucidation of bioactive compounds of which Raman spectroscopy, based on molecular vibrations, is emerging as an important nondestructive and useful analytical tool for biologic materials, including whole bacteria because of the high specificity and high resolution [1]. Earlier work on the isolation and purification of karanjin indicates that it is a challenge to achieve the compound in high purity due to its labile nature [2, 3]. This article mainly focuses on the isolation and structural characterization of karanjin. Techniques involved in this study are UV-Visible, FTIR, HRMS, FESEM, XRD, NMR, Raman spectroscopy, and TGA.

Finally, an *in vitro* study of the antibacterial action has been studied using the microbroth dilution assay, Raman spectroscopy, and electron microscopy. The effect of karanjin on the pathogenic bacteria was assessed by measurement of cell leakage and vibrational modes using Raman scattering. The results clearly demonstrated the in silico and *in vitro* antibacterial action of karanjin against pathogenic bacteria.

A compound was isolated from the ethyl acetate crude extract by column chromatography using a hexane-ethyl acetate eluent system. The compound was purified and the R_f value of the compound was found to be 0.44 in the hexane-ethyl acetate (85 : 15) eluent system. After crystallization, the colorless needle-shaped crystals with a melting point of 158 °C were obtained. The process of recovery through crystallization was very efficient in achieving a yield of pure crystals up to approximately 2%. The mass of the compound was confirmed by the HRMS having a molecular formula of $C_{18}H_{12}O_4$ (**Fig. 1**). The *m/z* of the isolated compound in the positive mode $[M + H]^+$ was 293.0879 (**Fig. 1 S**, Supporting Information) and the exact molecular mass was 293.0808, which matched well with the reported mass value of karanjin [2]. To ascertain the purity of karanjin isolated in this study, analytical HPLC was performed [4]. The compound showed a retention time of 17.68 min and 98% purity when compared

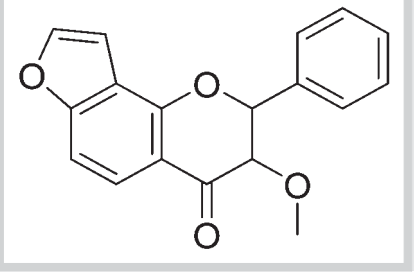

Fig. 1 Chemical structure of karanjin (3-methoxy-2-phenylfuro [2,3-h]chromen-4-one).

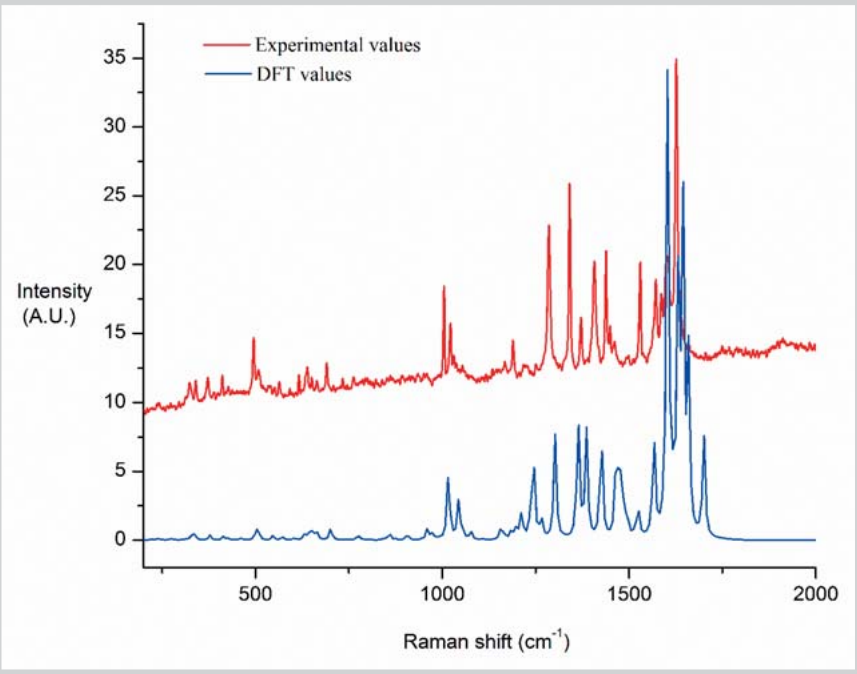

Fig. 2 Comparison of vibrational assignment of karanjin crystal experimental values by Raman spectrophotometer with calculated DFT values, peaks are well matched.

with standard karanjin (99%, Sigma-Aldrich) (**Fig. 2 S**, Supporting Information). The relative standard deviation for the retention time and peak area was less than 0.04% and 1.24%, respectively. Earlier reports with regards to karanjin isolation from the seeds varied from 1 to 1.5% depending upon the geographical site of collection with a maximum purity of 80% as evaluated by HPLC [3]. In the current study, the pure compound has been achieved by a single extraction step followed by purification with selected adsorbent and appropriate solvents during chromatography.

Karanjin was validated and confirmed by various types of spectroscopy, viz., FTIR (**Fig. 3 S**, Supporting Information) [5], NMR (**Fig. 4 S**, Supporting Information), XRD (**Fig. 5 S**, Supporting Information) [6–8], FESEM (**Fig. 6 S**, Supporting Information), and thermogravimetric analysis (**Fig. 7 S**, Supporting Information) [9].

The Raman spectrum of pure karanjin crystal along with the DFT calculation were carried out with Gaussian 09 software at the B3LYP/6–311 G (D, P) level [5]. DFT frequencies below 1500 cm^{-1} were scaled by a factor of 0.98 to provide the best fit to the spectrum. These scaled theoretical wavenumbers are in perfect agreement with the experimental values of pure karanjin crystal as shown in **Fig. 2**. The prominent peaks observed at 1605 cm^{-1} and 1627 cm^{-1} are due to strong C=O stretching of the flavone ring [10] and these peaks are in good agreement with the DFT calculated values, such as 1610 and 1631 cm^{-1} (**Table 1**). The peak at 1372 cm^{-1} present in the spectrum is due to the presence of a -CH_3 group. Another intense peak at 1005 cm^{-1} is due to the trigonal stretch of the flavone B ring. Furthermore, peaks at 1191, 1285, and 1530 cm^{-1} are involved in the bending of the CH plane. All these observed peaks in the Raman spectrum of karanjin matched well with three flavonoids, chrysin, apigenin, and leutin, and some flavones [10, 11]. A few other additional peaks at 1022, 1341, and 1438 cm^{-1} are due to the CH vibration in the furan ring and are in close agreement with DFT calculations.

The physicochemical parameters of karanjin were determined by using OSIRIS Property Explorer [12, 13]. A molecular docking study has also been undertaken to screen the possible target of action of karanjin among common target sites of bacteria [14, 15]. Further, the antibacterial activity of karanjin has been evaluated by the microbroth dilution assay and Raman spectroscopy against SA and ETEC at its MIC values (**Fig. 3**). The antimicrobial effectiveness is thought to come from flavonoids for their abilities to form complexes with both extracellular and soluble proteins as well as bacterial membranes. The activity of karanjin could be due to the presence of a hydrophilic substituent in the furan and flavonoid moieties, which is very important for antimicrobial effects [16–21].

Raman spectroscopy provided a fingerprint region below the wavenumber of 1800 cm^{-1}, which reflects detailed information about the composition of bacterial cells [22]. A high-intensity peak at 1007 cm^{-1} was observed due to C-C stretching of the aromatic ring. Furthermore, another intense peak signal was observed at 1525 cm^{-1}, which can be attributed to pigments of the carotenoid family, and at 1162 cm^{-1}, due to the presence of C-C

Table 1 Comparison between Raman vibrational frequencies of karanjin with theoretical DFT calculations.

Sr. no.	Raman Exp. (cm^{-1})	DFT Cal. (cm^{-1})
1	327	331
2	495	504
3	691	699
4	1005	1008
5	1022	1043
6	1191	–
7	1286	1246
8	1341	1305
9	1372	1388
10	1408	1424
11	1438	1426
12	1530	1526
13	1575	1566
14	1605	1610
15	1627	1631

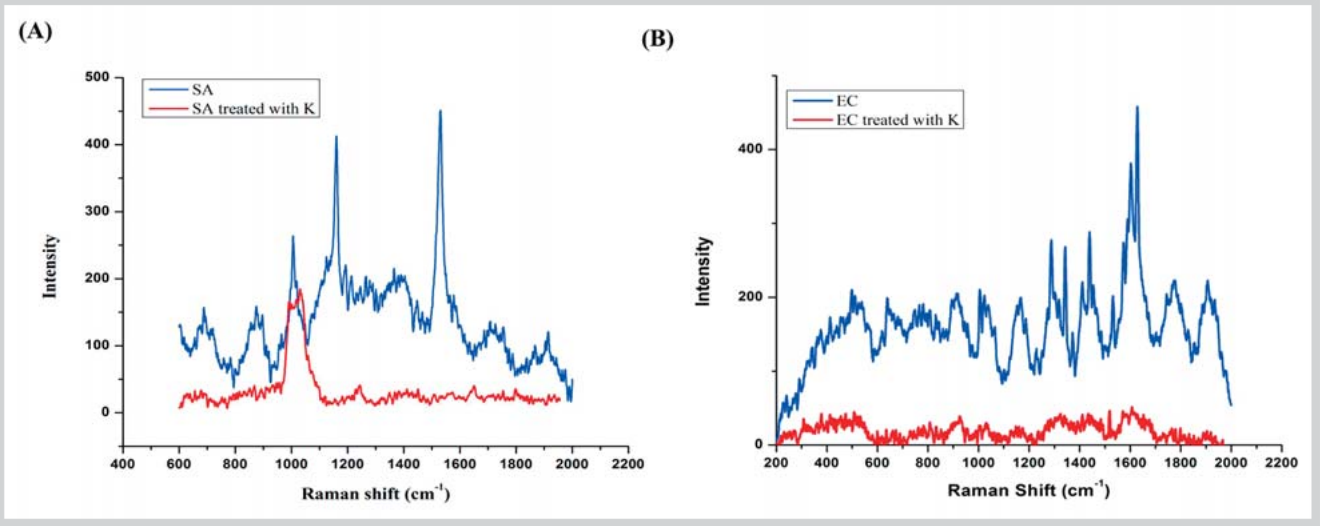

Fig. 3 Raman spectra of *S. aureus* (SA) and *E. coli* enterotoxic (ETEC) showing antibacterial action of karanjin (K) at their respective MICs. (Color figure available online only.)

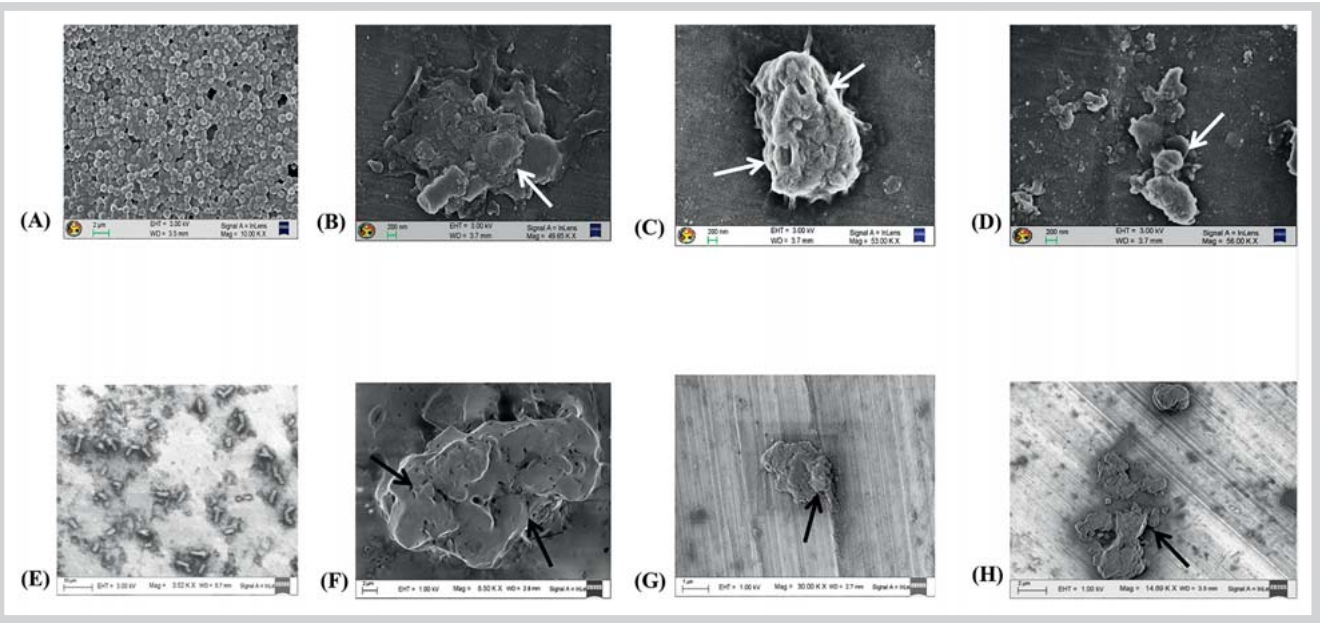

Fig. 4 Field emission scanning electron micrographs of *S. aureus* (**A**–**D**) and *E. coli* enterotoxic (**E**–**H**). **A** and **E** Untreated bacterial cells and bacterial cells after treatment with karanjin at their respective MICs. (Color figure available online only.)

conjugated stretching in the carotenoids. Peaks at 1455, 1606, and 1614 cm^{-1} in bacterial cells are assigned to the vibrations of tyrosine and phenylalanine of the proteins [1]. The bands at 1289 and 1342 cm^{-1} are assigned to L-glutamate and glycine, respectively, whereas the band at 1628 cm^{-1} is assigned to pyruvate in ETEC. The band at 1009 cm^{-1} present in the spectra of L-tryptophan can be assigned to the trigonal ring breathing of the benzene ring. On the other hand, the Raman spectra of linear saturated fatty acids present in ETEC cells show the band at 1438 cm^{-1} along with a few smaller bands [1]. The bands at 1598 cm^{-1} and 1320 cm^{-1} in SA are assigned to phenylalanine and guanine, respectively [23]. Moreover, SA and ETEC bacterial cells after treatment with karanjin signify cell lysis with a sharp decline in almost all prominent peak intensities.

The bacteria SA and ETEC were examined by FESEM to observe morphological changes caused by treatment with karanjin. FESEM images of untreated SA and ETEC showed an intact, smooth cell surface with defined cell features (**Fig. 4A, E**), whereas shrinking, membrane disintegration, and prominent damage of the cell wall was observed in bacterial cells treated with the compound (**Fig. 4B–D, F–H**). These findings indicate that karanjin caused the lysis of SA and ETEC by degrading the bacterial cell wall and affecting the cytoplasmic membrane [17, 24].

Materials and Methods

Plant material

The plant material used in the current study was seeds from an earlier characterized candidate plus tree (CPT) individual of Karanj, North Guwahati *Pongamia pinnata* 46 (NGPP 46) [25].

Isolation

Dried powdered seeds were subjected to a hot solvent in a Soxhlet apparatus using ethyl acetate in a ratio of 1 : 6 (wt./vol). To isolate karanjin, ethyl acetate crude extracts (2 g) were subjected to column chromatography on silica gel (80 g, 60–120 mesh, 3 × 60 cm glass column) and the compound was eluted gradually with an increasing polarity of hexane-ethyl acetate two-phase eluent systems.

Characterization and structural elucidation

Raman spectroscopy: The Raman spectrum of the pure isolated crystal was recorded by a Horiba model LabRAM HR spectrometer in the back scattering mode using an Argon-ion laser at a wavelength of 514 nm as the excitation source at room temperature and the signals were taken at specific wavenumbers (200 to 2000 cm^{-1}) [10].

Density functional theory: Recorded experimental data from micro-Raman and FITR were correlated with the reference to DFT (B3LYP/6–311 G **(**D, P**)** calculations using Gaussian 09 software [5] to determine the vibrational and rotational modes in the sample.

Antibacterial property

Bacterial strains: The antibacterial activity of the isolated compound was evaluated against two bacteria, viz., *Staphylococcus aureus*, SA (ATCC 6538) and *Escherichia coli* enterotoxic, ETEC (MTCC 723). All the tested bacteria were grown and maintained on nutrient agar (NA) as described earlier by [25].

Antibacterial study by Raman spectroscopy: Characterization of the bacterial cells before and after exposure of the compound was also performed on gram-positive bacteria, SA and gram-negative bacteria, ETEC using Raman spectroscopy. Untreated bacterial cells were used as a negative control. About 3 mL of bacterial cultures at the exponential growth phase (10^6 CFU/mL) were centrifuged at 3000 rpm for 5 min. Cells were washed and suspended in sterile distilled water. After that, the sample was put onto the coverslip and allowed to dry at 37 °C and then the spectrum was recorded for changes in the intensity and shift in the Raman spectrum [24].

FESEM

FESEM was used to visualize the changes in the morphology of the SA and ETEC cells before and after treatment with karanjin. Untreated bacterial cells were used as negative control. The bacterial samples were washed with 50 mM phosphate buffer solution (pH 7.2), fixed with 2.5% glutaraldehyde in PBS and rinsed with the same buffer. The specimen was dehydrated in ascending grades of ethanol concentrations ranging from 30% to 100%, coated with gold and then analysed through FESEM (Carl Zeiss, Ultra 55) as described in detail previously by Ghosh et al. [26].

Statistical analysis

All experiments were set up in a completely randomized design and repeated thrice with a minimum of three replicates. The statistical analysis was carried out using SPSS Statistics 17.0.

Supporting information

HRMS, HPLC, FTIR, NMR, XRD, FESEM, and TGA data of karanjin as well as *in silico* predictions of the drug likeness property, docking studies, and determination of MIC by the microbroth dilution assay are available as Supporting Information.

Acknowledgements

A.S., I.J., and M.S. thank MHRD, Government of India for student fellowships. Thanks to the Department of Biosciences and Bioengineering, IIT Guwahati, for providing a facility related to the spectroscopy. Thanks also to the Central Instruments Facility (CIF), IIT Guwahati, for providing various sophisticated analytical facilities. A.N.P. thanks the Department of Science and Technology, New Delhi, India (DST Project No. SB/S1/PC-035/2013) for research funding.

Conflict of Interest

The authors declare no conflict of interest.

References

1 *Naumann D.* FT-infrared and FT-Raman spectroscopy in biomedical research. Appl Spectrosc Rev 2001; 36: 239–298
2 Katekhaye SD, Kale MS, Laddha KS. A simple and improved method for isolation of karanjin from *Pongamia pinnata* Linn. seed oil. Indian J Nat Prod Resour 2012; 3: 131–134
3 *Vismaya W, Eipeson S, Manjunatha JR, Srinivas P, Kanya TCS.* Extraction and recovery of karanjin: A value addition to karanja (*Pongamia pinnata*) seed oil. Ind Crop Prod 2010; 32: 118–122
4 *Prabhu TM, Devakumar C, Sastry VRB, Agrawal DK.* Quantification of karanjin using high performance liquid chromatography in raw and detoxified karanj (*Pongamia Glabra* Vent) seed cake. Asian-Australas J Anim Sci 2002; 15: 416–420
5 *Frisch MJ, Trucks GW, Schlegel HB, Scuseria GE, Robb MA, Cheeseman JR, Montgomery jr. JA, Vreven T, Kudin KN, Burant JC, Millam JM, Iyengar SS, Tomasi J, Barone V, Mennucci B, Cossi M, Scalmani G, Rega N, Petersson GA, Nakatsuji H, Hada M, Ehara M, Toyota K, Fukuda R, Hasegawa J, Ishida M, Nakajima T, Honda Y, Kitao O, Nakai H, Klene M, Li X, Knox JE, Hratchian HP, Cross JB, Bakken V, Adamo C, Jaramillo J, Gomperts R, Stratmann RE, Yazyev O, Austin AJ, Cammi R, Pomelli C, Ochterski JW, Ayala PY, Morokuma K, Voth GA, Salvador P, Dannenberg JJ, Zakrzewski VG, Dapprich S, Daniels AD, Strain MC, Farkas O, Malick DK, Rabuck AD, Raghavachari K, Foresman JB, Ortiz JV, Cui Q, Baboul AG, Clifford S, Cioslowski J, Stefanov BB, Liu G, Liashenko A, Piskorz P, Komaromi I, Martin RL, Fox DJ, Keith T, Al-Laham MA, Peng CY, Nanayakkara A, Challacombe M, Gill PMW, Johnson B, Chen W, Wong MW, Gonzalez C, Pople JA.* Gaussian 03, Revision C.02. Wallingford, CT: Gaussian, Inc.; 2004
6 *Sheldrick GM.* SADABS. Göttingen, Germany: University of Göttingen; 2004
7 *Sheldrick GM.* SHELXL97 Program for crystal structure refinement. Göttingen, Germany: University of Göttingen; 1997
8 *Dolomanov OV, Bourhis LJ, Gildea RJ, Howard JAK, Puschmann H.* OLEX2: a complete structure solution, refinement and analysis program. J Appl Cryst 2009; 42: 339–341
9 *Gill PS, Sauerbrunn SR, Crowe BS.* High resolution thermogravimetry. J Therm Anal 1992; 38: 255–266
10 *Cañamares MV, Lombardi JR, Leona M.* Raman and surface enhanced Raman spectra of 7-hydroxylfavone and 3′,4′-dihydroxyflavone. e-PS 2009; 6: 81–88
11 *Corredor C, Teslova T, Cañamares MV, Chen Z, Zhang J, Lombardi JR, Leona M.* Raman and surface-enhanced Raman spectra of chrysin, apigenin and luteolin. Vib Spectrosc 2009; 49: 190–195
12 *Lipinski CA, Lombardo F, Dominy BW, Feeney PJ.* Experimental and computational approaches to estimate solubility and permeability in drug discovery and development settings. Adv Drug Deliv Rev 1997; 23: 4–25

13 *Ayati A, Falahati M, Irannejad H, Emami S.* Synthesis, *in vitro* antifungal evaluation and *in silico* study of 3-azolyl-4-chromanone phenyl hydrazones. Daru 2012; 20: 46
14 *Dundas J, Ouyang Z, Tseng J, Binkowski A, Turpaz Y, Liang J.* CASTp: computed atlas of surface topography of proteins with structural and topographical mapping of functionally annotated residues. Nucleic Acids Res 2006; 34: 116–118
15 *Volkamer A, Kuhn D, Grombacher T, Rippmann F, Rarey M.* Combining global and local measures for structure-based druggability predictions. J Chem Inf Model 2012; 52: 360–372
16 *Yang B, Kotani A, Arai K, Kusu F.* Estimation of the antioxidant activities of flavonoids from their oxidation potentials. Anal Sci 2001; 17: 599–604
17 *Cowan MM.* Plant products as antimicrobial agents. Clin Microbiol Rev 1999; 12: 564–586
18 *Fowler Z, Baron GM, Panepinto JG, Koffas MA.* Melanization of flavonoids by fungal and bacterial laccase. Yeast 2011; 28: 181–188
19 *Kharb R, Shama P, Yar MS.* Pharmacological significance of triazole scaffold. J Enzyme Inhib Med Chem 2011; 26: 1–21
20 *Xu HX, Lee SF.* Activity of plant flavonoids against antibiotic-resistant bacteria. Phytother Res 2001; 15: 39–43
21 *Jeong MR, Park PB, Kim DH, Jang YS, Jeong HS, Choi SH.* Essential oil prepared from *Cymbopogon citratus* exerted an antimicrobial activity against plant pathogenic and medical microorganisms. Mycobiology 2009; 37: 48–52
22 *Movasaghi Z, Rehman S, Rehman IU.* Raman spectroscopy of biological tissues. Appl Spectrosc Rev 2007; 42: 493–541
23 *Maquelin K, Kirschner C, Choo-Smith LP, van den Braak N, Endtz HP, Naumann D, Puppels GJ.* Identification of medically relevant microorganisms by vibrational spectroscopy. J Microbiol Methods 2002; 51: 255–271
24 *Dutta RK, Sharma PK, Pandey AC.* Assessing the conformational and cellular changes of ZnO nanoparticles impregnated *Escherichia coli* cells through molecular fingerprinting. Adv Mat Lett 2011; 2: 268–275
25 *Kesari V, Das A, Rangan L.* Physico-chemical characterization and antimicrobial activity from seed oil of *Pongamia pinnata*, a potential biofuel crop. Biomass Bioenergy 2010; 34: 108–115
26 *Ghosh S, Indukuri K, Bondalapati S, Saikia AK, Rangan L.* Unveiling the mode of action of antibacterial labdane diterpenes from *Alpinia nigra* (Gaertn.) B. L. Burtt seeds. Eur J Med Chem 2013; 66: 101–105

received December 15, 2015
revised March 8, 2016
accepted March 10, 2016

Bibliography
DOI http://dx.doi.org/10.1055/s-0042-105159
Planta Med Lett 2016; 4: e91–e95

ISSN 2199-157X

Correspondence
Prof. Dr. Latha Rangan
Department of Biosciences and Bioengineering
Indian Institute of Technology Guwahati
Guwahati 781039, Assam
India
Phone: + 91 0 36 12 58 22 14
Fax: + 91 0 36 12 58 22 49
latha_rangan@yahoo.com